Holo-TFIID controls the magnitude of a transcription burst and fine-tuning of transcription

Katie L. Pennington, Sharon K. Marr, Gung-Wei Chirn, and Michael T. Marr II[1]

Department of Biology and Rosenstiel Basic Medical Sciences Research Center, Brandeis University, Waltham, MA 02454

Edited by Robert Tjian, Howard Hughes Medical Institute, Chevy Chase, MD, and approved March 27, 2013 (received for review December 12, 2012)

Transcription factor (TF)IID is a central player in activated transcription initiation. Recent evidence suggests that the role and composition of TFIID are more diverse than previously understood. To investigate the effects of changing the composition of TFIID in a simple system, we depleted TATA box-binding protein–associated factor (TAF)1 from *Drosophila* cells and determined the consequences on metal-induced transcription at an inducible gene, metallothionein B. We observe a marked increase in the levels of both the mature message and pre-mRNA in TAF1-depleted cells. Under conditions of continued metal exposure, we show that TAF1 depletion increases the magnitude of the initial transcription burst but has no effect on the timing of that burst. We also show that TAF1 depletion causes delay in the shutoff of transcription upon removal of the stimulus. Thus, TAFs are involved in both establishing an upper limit of transcription during induction and efficiently turning the gene off once the inducer is removed. Using genome-wide nascent sequencing, we identify hundreds of genes that are controlled in a similar manner, indicating that the findings at this inducible gene are likely generalizable to a large set of promoters. There is a long-standing appreciation for the importance of the spatial and temporal control of transcription. Here we uncover an important third dimension of control: the magnitude of the response. Our results show that the magnitude of the transcriptional response to the same signaling event, even at the same promoter, can vary greatly depending on the composition of the TFIID complex in the cell.

heavy metal | MtnA | coactivator | RNA polymerase

Transcription activation of protein-coding genes requires the regulated assembly of a large macromolecular complex termed the preinitiation complex (PIC) around the transcription start site (TSS). Major components of this complex are the general transcription factors (TFs) TFIIA, TFIIB, TFIID, TFIIE, TFIIF, and TFIIH, and the enzyme itself is RNA polymerase II (RNAP II). A central player in the assembly of the PIC is the TFIID complex, which nucleates the formation of the entire complex. In addition to being a general transcription factor, TFIID also serves as a coactivator required for response to transcriptional activators in metazoan cells. TFIID purified from rapidly growing cells contains the TATA box-binding protein (TBP) and 13 TBP-associated factors (TAFs) (1–3).

The TFIID complex is required for activated transcription by several classes of activators at both TATA-containing and TATA-less promoters (4). Upon recruitment by an activator, TFIID subunits bind to core promoter elements surrounding the TSS, including the TATA box, initiator (Inr), and downstream promoter element (DPE). This binding nucleates formation of the PIC. TBP binds to the TATA box, whereas the Inr and DPE are bound by TAFs (5–8). TBP has been shown to promote TATA-dependent transcription over DPE-dependent transcription, whereas the TBP-antagonizing proteins modifier of transcription 1 and negative cofactor 2 (NC2) have the opposite effect (9). A DPE-dependent promoter is immune to TBP depletion but sensitive to TAF4 depletion (9). This suggests alternate roles for TFIID subunits in facilitating transcription activation.

In addition to the diverse roles in transcription activation, recent work suggests that TFIID itself is much more complex and dynamic than previously thought (10). There are tissue-specific forms of TFIID required for proper tissue development and function (11, 12). TAF expression is lost in some differentiated cell types, including hepatocytes, myotubes, and *Drosophila* wings (13–15). Although the canonical TAFs are essential for proliferating cells, they are not essential for survival or even proliferation-independent differentiation of postmitotic cells (16, 17). Consistent with this finding, depletion or inactivation of some of the TAFs causes cell-cycle arrest (18–21). Finally, it appears that embryonic stem cells contain a noncanonical TFIID complex lacking several of the core subunits (22).

TFIID participates in the heavy metal-dependent induction of *Drosophila melanogaster* metallothionein genes in a noncanonical fashion (23). Expression of metallothionein A (MtnA) requires TBP, but depletion of TAF subunits using RNAi in *Drosophila* Schneider line 2 (S2) cells leads to an increase in MtnA expression levels, rather than the decrease in expression expected for a TFIID-bound gene (23). *Drosophila* somatic cells express a single homolog of each of the TAFs (24), and RNAi is efficient in S2 cells (25). This, combined with an easily observable TFIID effect, provides a simple system to investigate transcription dynamics under conditions of altered TFIID in the same cell type receiving the same signal.

In the current work, we examine the role of the intact TFIID complex in transcription dynamics by assessing the effect of TAF1 depletion on two metal-inducible genes, MtnA and MtnB, in *Drosophila* cells. We chose TAF1 depletion because it leads to the least invasive change in TFIID. TAF1 depletion leads to an untethering of TBP from the TAFs while leaving the levels of the core TAFs unchanged (26). In addition, TAF1 is not present in other TAF-containing complexes such as the Spt-Ada-Gcn5-Acetyl transferase complex (SAGA) (27). We observe a marked increase in MtnB expression levels by reverse transcription followed by quantitative PCR (RT-qPCR) of pre-mRNA transcripts in TAF1-depleted cells compared with mock-treated cells, both during continued induction and following removal of the inducer. Under conditions of continued metal exposure, we observe that TAF1 depletion increases the magnitude of the initial transcription burst but has no effect on the timing of that burst. We also observed that TAF1 depletion causes a delay in the shutoff of MtnB and MtnA transcription upon removal of the heavy metal. Thus, TAFs are involved in both establishing an upper limit of transcription during induction and efficiently turning the gene off once the inducer is removed. Genome-wide nascent sequencing (nascent-seq) data identified hundreds of genes that are controlled in a similar manner, indicating that the observations at this inducible gene are generalizable to a large set of promoters.

Author contributions: K.L.P., S.K.M., and M.T.M. designed research; K.L.P., S.K.M., and M.T.M. performed research; K.L.P., S.K.M., and M.T.M. contributed new reagents/analytic tools; K.L.P., S.K.M., G.-W.C., and M.T.M. analyzed data; and K.L.P., S.K.M., and M.T.M. wrote the paper.

The authors declare no conflict of interest.

This article is a PNAS Direct Submission.

Data deposition: The microarray and deep-sequencing data reported in this paper have been deposited in the Gene Expression Omnibus GEO database, www.ncbi.nlm.nih.gov/geo (accession no. GSE45873).

[1]To whom correspondence should be addressed. E-mail: mmarr@brandeis.edu.

This article contains supporting information online at www.pnas.org/lookup/suppl/doi:10.1073/pnas.1221712110/-/DCSupplemental.

Results

Depletion of TAF Subunits Leads to an Increase in both MtnA and MtnB mRNA Levels Following Exposure to Either Copper or Cadmium. We used RT-qPCR to detect endogenous transcript levels for two inducible genes, MtnA and MtnB, following depletion of TFIID subunits in *Drosophila* S2 cells. Cells were treated with dsRNA-targeting subunits of TFIID and then exposed to conditions of excess copper (Cu) or cadmium (Cd). As observed previously, MtnA transcript levels increase following Cu exposure in TAF-depleted cells, but the expression depends on TBP (Fig. 1*A*) (23). A similar result is seen for the MtnB transcript following copper induction (Fig. 1*B*). We have shown that MtnA and MtnB have a differential response to the nature of the metal insult in S2 cells (28). The requirement for TBP, but not the TAFs, is not metal-dependent, as a similar result is found for both MtnA and MtnB transcripts following induction with cadmium (Fig. 1 *C* and *D*).

The magnitude of the TAF effect does depend on the metal type and the promoter. The greatest increase in transcripts caused by TAF depletion is observed at the MtnB gene following induction with Cu (Fig. 1*C*). Thus, the MtnB gene has a larger dynamic range with which to examine this noncanonical role for the TAFs. In addition, MtnB provides a good model for activation because it has extremely low basal levels of expression. To determine whether this was the result of a paused polymerase or whether it is a classic example of an inactive gene lacking RNA polymerase, we performed chromatin immunoprecipitation followed by microarray analysis (ChIP-chip) using antibodies directed against RNAP II (23). We also compared our results to results from the modENCODE project using publicly available data (29). Both sets of experiments show that whereas MtnA has readily detectable levels of RNAP II bound at the gene in the absence of metal shock, no RNAP II is detectable at the MtnB locus under these same conditions (Fig. 1 *E* and *F*). Additionally, the MtnB transcript is undetectable in deep sequencing of nascent RNA in uninduced cells (see below).

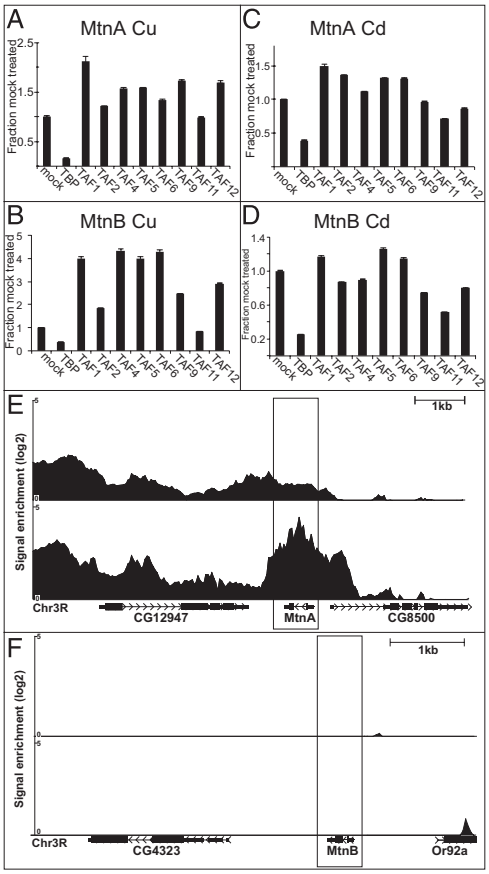

Fig. 1. *D. melanogaster* metallothionein A and B expression following depletion of TBP and TAF subunits. S2 cells treated with dsRNA targeting TFIID or mock-treated were induced with Cu or Cd and mRNA levels were measured by RT-qPCR. MtnA (*A* and *C*) and MtnB (*B* and *D*) expression was determined by RT-qPCR and normalized to the ribosomal protein (RP)49 transcript. Values shown are fractions of the mock-treated samples. Error bars represent SE of qPCR triplicates. Experiments were repeated in at least two independent biological replicates, and data are consistent with those shown. (*E*) RNAP II occupancy at MtnA in untreated S2 cells. (*Upper*) Data signal enrichment in immunoprecipitation versus input in our S2 cells. (*Lower*) Analysis of publicly available modENCODE data for comparison. (*F*) RNAP II occupancy at MtnB in untreated S2 cells as in *E*.

Going forward, we chose to use TAF1 depletion to investigate the basis for the increase in mRNA levels for a number of reasons. TAF1 is efficiently depleted in S2 cells (Fig. S1*A*) (23, 26). Depletion of TAF1 results in the most moderate effects on TFIID overall. It disrupts the TFIID complex by untethering TBP from the core TAFs but does not result in the loss of the other TAFs from these cells (Fig. S1*B*) (26). Additionally, TAF1 is not present in other TAF-containing complexes such as SAGA, so the effects should be limited to TFIID. To verify that the increased transcript levels are not an off-target dsRNA effect, we depleted TAF1 and expressed an RNAi-resistant TAF1 by transient transfection. Because transfection efficiency is low in these cells, we used a reporter construct expressing the firefly luciferase ORF under the control of the MtnB promoter. When the RNAi-resistant TAF1 was expressed in cells depleted of endogenous TAF1, the increase in luciferase activity compared with mock-treated cells was no longer observed (Fig. S2). This demonstrates that the increase in transcript levels following TAF1 depletion is the specific effect of TAF1 depletion, and not an off-target effect.

TAF1 Depletion Affects the Magnitude, but Not the Timing, of the Initial Transcription Burst at MtnB. To determine the dynamics of the TAF1 depletion effect at the MtnB gene following metal induction, we heavy metal-shocked TAF1-depleted and mock-treated cells with Cu. Samples for RT-qPCR were removed at the times indicated. The MtnB mRNA levels in the TAF1-depleted cells are increased relative to the mock-treated cells at all time points tested after induction (Fig. 2*A*). Similar results were obtained when Cd was used (Fig. S3).

To determine whether this was a direct effect on transcription of the MtnB gene, we used primers specific for the intron-containing MtnB pre-mRNA nascent transcripts. Most splicing in *Drosophila* occurs cotranscriptionally (30), so the levels of pre-mRNA closely reflect nascent transcripts and thus the levels of active RNAP II on the gene at the time of sample collection. MtnB pre-mRNA levels are shown in Fig. 2*B*. For both TAF-depleted and mock-treated cells the pre-mRNA transcript levels initially burst, peaking at 1 h following metal addition, and then decrease to a lower-level intermediate between the basal and the peak burst level, plateauing at about 4 h following induction. These kinetics are reminiscent of the burst-attenuation kinetics seen at other signal-inducible genes.

MtnB pre-mRNA levels are increased in TAF1-depleted cells relative to mock-treated cells throughout the induction time course, including both the transcriptional burst and the maintenance phase. To determine whether TAF1 depletion also affects the timing of the burst, we normalized the MtnB pre-mRNA data for both mock-treated and TAF1-depleted samples to the peak time point (Fig. 2*C*). The resulting curves are almost superimposable, illustrating that there is no change in the timing of the burst following metal addition in TAF1-depleted cells compared with mock-treated cells; only the magnitude of the burst changes.

To determine whether the effects observed with nascent RNA reflected TBP recruitment or RNA polymerase occupancy, we performed chromatin immunoprecipitation with antisera against

BIOCHEMISTRY

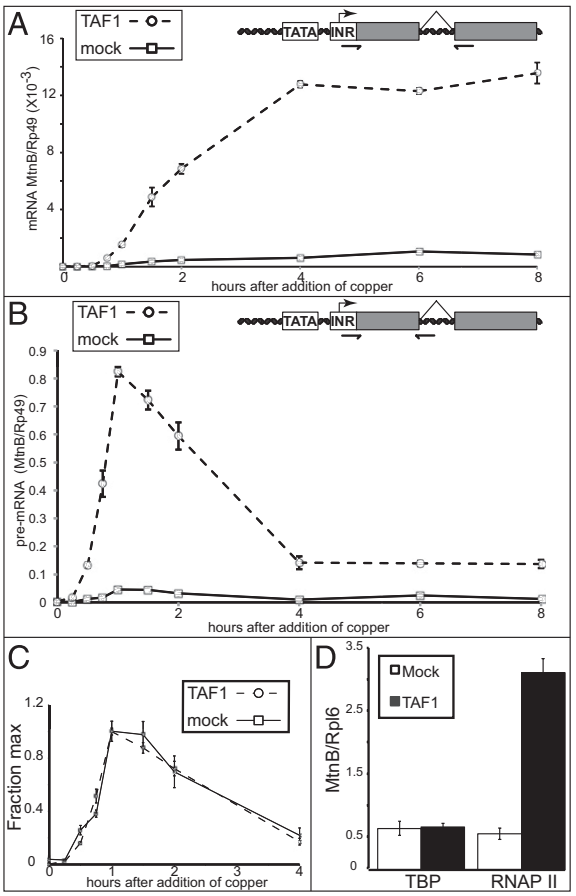

Fig. 2. Induction of MtnB following addition of Cu. S2 cells treated with TAF1 dsRNA or mock-treated were induced with Cu for the indicated times and RNA levels were measured by RT-qPCR. (*A*) MtnB mature mRNA normalized to RP49. (*B*) MtnB intron-containing pre-mRNA normalized to RP49 intron-containing pre-mRNA. Primer binding sites are indicated by the arrows in the gene diagrams above the graphs. (*C*) MtnB pre-mRNA levels plotted as a fraction of the 1-h time point. Error bars are SEMs of qPCR. (*D*) ChIP of TBP or RNA polymerase II at the MtnB promoter at 80-min treatment with copper. Data are plotted as the precipitation relative to the housekeeping gene RPL6. All experiments were repeated in two independent biological replicates, and data are consistent with those shown.

TBP or RNAP II at the peak time point of nascent RNA synthesis. To control for ChIP efficiency, we determined the amount of TBP and RNA polymerase relative to a housekeeping gene that is unaffected by TAF1 depletion (see below). We find no difference in the amount of DNA precipitated relative to the control using the TBP antisera (Fig. 2*D*). By contrast, DNA precipitated by the RNAP II antisera indicates an increase in RNAP II at MtnB when TAF1 is depleted (Fig. 2*D*). This is consistent with the increase in intron-containing MtnB RNA observed under these conditions.

TAF1 Depletion Results in Delayed Shutoff of MtnB and MtnA Following Removal of Copper Inducer. Depletion of TAF1 from these cells increases the levels of nascent transcripts and RNAP II loading onto the MtnB gene following metal shock. This suggests that TFIID functions as a governor at this gene setting an upper limit to transcription. To determine whether the TFIID governor function plays a role in turning off the gene following removal of metal, we performed shutoff experiments. TAF1-depleted or mock-treated cells were induced with Cu for 90 min. The Cu was then chelated using the Cu-specific chelator bathocuproine sulfonate (BCS) and the cells were washed to remove the chelated complex. Samples were removed and processed for RT-qPCR at the indicated time points (Fig. 3*A*). MtnB pre-mRNA levels are greater in TAF1-depleted cells than in mock-treated cells, both before and after washout (Fig. 3*B*). To compare the timing of the shutoff, the data are plotted as a fraction of the peak time point. MtnB pre-mRNA levels show a delay in the drop-off in TAF1-depleted cells compared with mock-treated cells (Fig. 3*C*). TAF1 depletion results in a roughly 15-min delay in the shutoff of the MtnB gene following removal of inducer. Similar results are obtained at the MtnA gene (Fig. S4). This suggests that TFIID has a role in both determining the upper limit of transcription upon metal induction and shutting off the gene once the metal inducer is removed.

Genome-Wide Analysis of Nascent RNA Indicates Gene Expression Control by TFIID Composition Is Widespread. To determine how common the effects of TAF1 depletion are, we identified genes that have increased or decreased nascent RNA levels in TAF1-depleted cells under normal growth conditions. Transcripts were identified using the nascent-seq technique (30). This technique is based on the stability of the RNAP II elongation complex. Chromatin-associated transcripts are purified under high-stringency conditions that select for only nascent RNAs associated with an elongating polymerase (31). The nascent RNAs are reverse-transcribed and sequenced using a strand-specific deep-sequencing

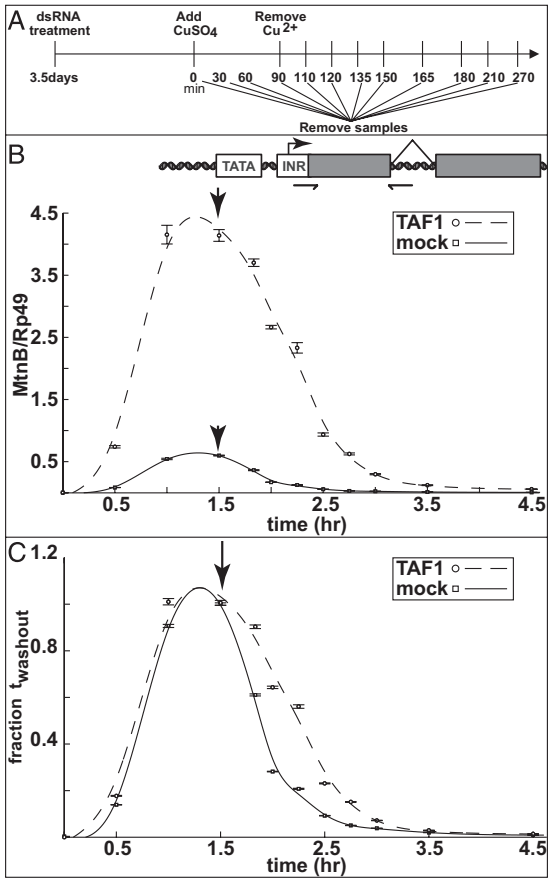

Fig. 3. Shutoff of MtnB pre-mRNA expression following removal of stimulus. (*A*) S2 cells treated with TAF1 dsRNA or mock-treated were induced with Cu for 1.5 h. Cu was then chelated with BCS. Cells were washed twice with media containing BCS and then incubated in complete media for the indicated times. (*B*) MtnB pre-mRNA expression normalized to RP49 pre-mRNA levels. (*C*) Normalized MtnB pre-mRNA levels plotted as a fraction of the 1.5-h time point for both washout conditions. Error bars represent SEMs. Two independent biological replicates were performed and results were comparable. Arrows indicate time of washout.

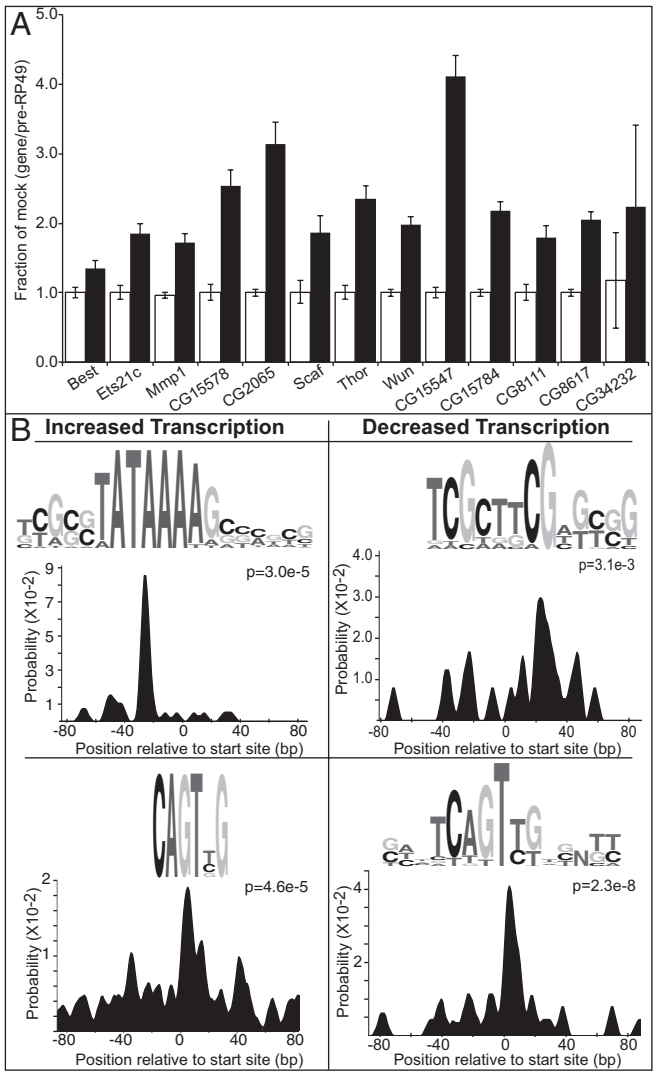

Fig. 4. Genome-wide analysis of nascent RNA in TAF1-depleted cells. (*A*) RT-qPCR validation of 13 genes identified in the initial nascent-seq dataset. (*B*) Motifs identified as overrepresented in the promoters of genes showing either increased transcription or decreased transcription by nascent-seq.

protocol on the Illumina platform. The reads are then mapped to the *Drosophila* reference genome.

Comparisons of reads per kb per million mapped reads (RPKM) from the mock-treated cells with the RPKM from TAF1-depleted cells identified a number of genes whose nascent RNA reads increase. To validate this approach, we tested 13 genes identified in the first round of deep sequencing by RT-qPCR in a second biological replicate. All of the genes showed an increase in nascent RNA in the biological replicate (Fig. 4*A*), indicating that the approach was valid. Encouraged by these results, we also deep-sequenced the nascent RNA from the second biological replicate.

We identified 369 genes that reproducibly showed a greater than 50% increase in nascent RNA in TAF1-depleted cells (Table S1; example in Fig. S5), about 5.7% of detectable active genes. Additionally, we identified 115 genes that reproducibly showed a decrease in nascent RNA in TAF1-depleted cells representing about 1.8% of detectable genes (Table S2; example in Fig. S5).

We used each of these datasets in an attempt to identify sequence motifs that might be important for the transcriptional response to TAF1 depletion. We took the DNA sequence of the 200 bp centered on the annotated transcription initiation site for each of the genes in each of the lists and used the MEME suite to identify overrepresented motifs (32). Fig. 4*B* shows the motifs enriched for both the increased and decreased genes. In addition to identification of the motifs, we used the CentriMo algorithm to determine whether there was a preferred position around the start site of transcription (33).

For genes with increased nascent RNA, two motifs were identified as both overrepresented and positionally constrained. A motif resembling the TATA element is overrepresented (Fisher exact test, $P = 1.2 \times 10^{-14}$). This motif was present in 36.6% of the genes identified as having increased nascent RNA. By comparison, the TATA element is present in only 5% of *Drosophila* promoters genome-wide (34). In addition, this motif is found preferentially in the −25 to −30 position relative to the start site of transcription in this dataset, an appropriate position for the TATA element. The second motif identified as overrepresented (Fisher exact test, $P = 8.5 \times 10^{-15}$) in the dataset resembles the initiator element CAGT. It is found in 36% of the sequences in the dataset compared with 15% of *Drosophila* promoters genome-wide (34). This element shows a preference for positioning around the start site of transcription.

For the genes with decreased nascent RNA, two sequence motifs were identified as both overrepresented and showing positional constraints. A motif resembling the Inr is overrepresented (Fisher exact test, $P = 5.1 \times 10^{-7}$). This motif was present in 27% of the genes identified as having decreased nascent RNA. This motif is found enriched in the region around the start site of transcription. The second motif identified as overrepresented (Fisher exact test, $P = 3.0 \times 10^{-3}$) in the decreased dataset resembles a DPE. It is found in 14% of the sequences in the dataset, compared with 2% of *Drosophila* promoters genome-wide (34). This motif is found preferentially just downstream of the start site of transcription in a position appropriate for the DPE.

Using the motifs defined as specific for the TAF1 effects, we asked how many of the genes containing these motifs are affected. Our nascent-seq data identify 6,436 genes that are transcribed in our S2 cells. Using the TATA motif, we identified 204 transcribed genes that contain a sequence matching the motif; 41 of these are affected by TAF1 depletion. Using the same type of analysis for the DPE motif, we find 314 genes that contain the motif; 33 of these genes are affected by TAF1 depletion.

Discussion

The noncanonical activity of TAFs at the MtnB gene appears to have a dual role in both imposing an upper limit to the activated transcription by limiting the loading of RNA polymerase onto the gene and ensuring efficient shutoff of the gene following removal of stimulus. It may be that this allows the cells to more finely tune the transcriptional response and prevent overaccumulation of a target transcript. TAFs may impose a rate-limiting step that serves as a checkpoint to ensure continued activator signaling or proper PIC assembly. Given that TFIID has been known to exist in multiple conformers that footprint across the TSS (reviewed in ref. 35) and that a slow isomerization of TFIID has been shown to be rate-limiting for pol II transcription in vitro (36), it seems reasonable that this step may be rate-limiting at a subset of promoters in vivo. Therefore, eliminating this rate-limiting step by depleting TAFs from the cell may facilitate a higher transcription-initiation rate.

In the current work, we show that a transcriptional coactivator is central to determining the upper limit of an initial transcriptional burst in response to a signal. Although this is an ensemble observation, work on single cells shows that an increase in transcription output is often derived from a change in the amount of bursting of individual alleles. Others have shown that changing the amount of activator affects the magnitude of each of these microbursts observed from doxycycline-controllable promoters in CHO cells, but not the frequency of the microbursts (37). It seems reasonable, therefore, that activator-dependent processes would also exhibit similar effects. That is, changes to processes functioning downstream of activator binding to the promoter would be expected to

modulate the magnitude of transcriptional bursts without affecting the frequency of those bursts. This suggests that depletion of TAF1 results in increased efficiency of activator-dependent processes, and does not appear to affect the processes controlling the timing of the burst, which may involve changes in metal-responsive transcription factor 1 (MTF-1) signaling or in chromatin accessibility.

Genome-wide analysis of nascent RNA using nascent-seq reveals hundreds of genes that are affected by TAF1 depletion. The promoters of genes whose nascent RNA increases in the TAF1-depleted cells are enriched for a motif resembling the TATA box. Consistent with this finding, both MtnA and MtnB, the original model promoters, contain a TATA box and show an increase in transcription in TAF1-depleted cells (23, 26). Because TAF1 depletion in *Drosophila* S2 cells leads to a separation of the TAF complex from TBP (Fig. S1*B*) (26), this result is in good agreement with previous findings that an increase in free TBP favors expression from TATA-containing promoters (9). Genes that have less nascent RNA in the TAF1-depleted cells are enriched for promoters containing a DPE. This is consistent with the notion that the TAFs are involved in binding the DPE and that a stable interaction with TBP is required for DPE function (6). In addition, this genome-wide finding is in good agreement with reporter assays that show TAF1 depletion has a strong negative affect when a MtnA hybrid promoter is driven by a DPE (26).

It is important to note that although the effects of TAF1 depletion are seen at hundreds of genes, we did not identify every TATA-containing gene as up-regulated nor every DPE gene as down-regulated. The specific activators and signals controlling many of these genes are unknown, but this result implies that some activators are more dependent on an intact TFIID than others. This also suggests that the interplay between the sequence-specific DNA-binding proteins and the TFIID complex is important in the context of the core promoter.

The observation that TFIID subunits can have a repressive role at a subset of genes speaks to the complexity of transcriptional regulations used by cells to maintain appropriate levels of gene expression. Our experiments highlight the importance of both the core promoter and the composition of the TFIID complex in the magnitude of a transcriptional response to signaling events. Given the recent data on the diversity of the TFIID complex in different cell types, it is reasonable to believe that the level of activation of a target gene, even to the same signal, will depend on the TFIID composition. There is a long-standing appreciation for the importance of the spatial and temporal control of transcription. Here we are implicating an important third dimension of control, the magnitude of the response. Many questions still remain regarding the dynamics of transcription and the varied roles of TAFs in facilitating an appropriate response to cellular signals.

Materials and Methods

dsRNA Production. TAF and TBP RNAi were the same as in refs. 23 and 26. The mock sequence is the *Escherichia coli lacI* ORF. For RNAi-resistant TAF1 experiments, the dsRNA targeted the 5′ and 3′ UTR of the endogenous TAF1 transcript. Transcription templates were PCR-amplified from plasmids using T3 and T7 primers. Templates were transcribed using either T3 or T7 RNA polymerase. The RNAs were annealed by mixing equal amounts of each ssRNA, incubating at 95 °C for 2 min followed by 60 °C for 30 min, and then cooling to 25 °C.

Cell Culture and RNAi. *D. melanogaster* Schneider line 2 cells were maintained at 25 °C in Schneider's medium containing 10% (vol/vol) FBS, 100 units/mL penicillin, and 0.1 mg/mL streptomycin. RNAi was performed as described (25) for 1 h in serum-free media before addition of Chelex 100-treated complete media. Cells were incubated with dsRNA for 3.5 d. For metal treatment, cells were induced with either 0.5 mM $CuSO_4$ or 0.05 mM $CdCl_2$ for the indicated times. Cells were harvested by scraping.

RT-qPCR. RNA extraction was performed using RNeasy Mini Kits (QIAGEN) according to manufacturer instructions. The RNA was digested with DNase I and first-strand cDNA synthesis was performed using either Moloney murine leukemia virus reverse transcriptase (MMLV-RT) or superscript III RT with random hexamers. The cDNA was digested with RNase H. qPCR was performed on diluted cDNAs using Promega GoTaq qPCR Master Mix and specific primers (600 nM) directed against each target transcript (Table S3) on a Chromo4 thermocycler (Bio-rad).

Chromatin Immunoprecipitation. Chromatin immunoprecipitation was performed as described (23) using polyclonal goat antisera raised against purified *Drosophila* RNA polymerase II (a generous gift of Arno Greenleaf, Duke University, Durham, NC) or polyclonal rabbit antisera against TBP (a generous gift of Jim Kadonaga, University of California at San Diego, La Jolla, CA). For tiling array analysis, precipitated DNA was labeled and hybridized to Affymetrix *Drosophila* tiling arrays as described (38). Replicate experiments were completed for all ChIP arrays. The profiles for each replicate dataset were combined using Affymetrix tiling analysis software. Combined input arrays were used to set the background signal intensities for the ChIP arrays. Data were visualized using the Integrated Genome Browser (39). The .CEL files generated by the modENCODE project for RNAP II ChIP-chip in S2 cells (DCCid:modENCODE_329) were downloaded and analyzed in the same manner as the in-house experiments using the Affymetrix tiling analysis software.

For quantitative PCR analysis, precipitated DNA was measured using SYBR Green in a Chromo4 thermocycler. Five microliters of precipitated DNA or input DNA was used in a 20-μL PCR containing 20 mM Tris·HCl (pH 8.8), 10 mM $(NH_4)_2SO_4$, 10 mM KCl, 2 mM $MgSO_4$, 0.1% Triton X-100, 200 μM dNTPs, 1 U Taq polymerase, 0.005 U pfu polymerase, 0.5 μM each primer, and 0.5× SYBR Green.

Washout. Cells were induced with 0.5 mM $CuSO_4$ for 90 min, and then treated with 2 mM BCS, pelleted, and washed twice with Chelex 100-treated complete media containing 1 mM BCS. After washing, the cells were resuspended in Chelex 100-treated complete media lacking BCS and divided into 35-mm dishes for incubation at 25 °C. Cells were harvested at the indicated time points for RNA extraction followed by RT-qPCR analysis. Data were normalized to RP49 pre-mRNA and curves were fit to the data using the Matlab R2012b (8.0.0) curve-fitting tool (MathWorks).

Nascent-Seq. S2 cells were treated with 40 μg/mL of dsRNA against TAF1 or *lacI* for 1 h in the absence of serum. Complete medium was replaced and cells were harvested after 4 d. Cells (6×10^7) were pelleted (1,500 × *g*) and washed once with cold 1× PBS. Nascent RNA was harvested using the NUN RNA isolation protocol as described (30) with the following addition: after lysis and dounce homogenization in buffer AT (15 mM Hepes·KOH, pH 7.6, 10 mM KCl, 5 mM MgOAc, 3 mM $CaCl_2$, 300 mM sucrose, 0.1% Triton X-100, 1 mM DTT, 1× SIGMAFAST), nuclei were pelleted at 1,000 × *g* for 5 min and resuspended in 1 mL of fresh buffer AT before layering on buffer B (15 mM Hepes·KOH, pH 7.6, 10 mM KCl, 5 mM MgOAc, 3 mM $CaCl_2$, 1 M sucrose, 1 mM DTT, 1× SIGMAFAST). RNA was purified from pellets in 1 mL of TRI Reagent (MRC).

Ribosomal RNA was depleted from 6 μg of nascent RNA as follows: 950 pmol of a mixture of biotinylated oligos targeting ribosomal RNA (Table S3) was bound to 0.6 mL of MagneSphere beads (Promega). The beads were washed four times with 0.5× SSC containing 10 mM EDTA. Oligo-bound beads were combined with nascent RNA in 2× SSC, 10 mM EDTA and heated at 68 °C for 10 min followed by incubation at 25 °C for 15 min and held on ice for 2 h with periodic mixing. Ribosomal-depleted RNA was collected. Beads were washed once with 0.5× SSC, 10 mM EDTA. Ribosomal-depleted RNA from the supernatant and wash were combined and precipitated with alcohol.

Libraries were constructed from 400 ng of ribosomal-depleted nascent RNA. RNA (40 μL) was fragmented at 65 °C for 5 min in 25 mM sodium carbonate (pH 9.2), 1 mM EDTA. Fragmentation was stopped by adding 190 μL of 0.33 M NaOAc (pH 5.2) followed by column purification (RNA Clean & Concentrator-5; Zymo Research). First-strand synthesis was primed with a random-tailed adapter (sm193). Reactions contained 50 mM Tris (pH 8.3), 75 mM KCl, 3 mM $MgCl_2$, 5 mM DTT, 0.5 mM dNTP, 2.5 μM primer, and 200 U MMLV-RT. Following reverse transcription, RNA was degraded with RNase H, and cDNA was column-purified (DNA Clean & Concentrator-5; Zymo Research). Second-strand synthesis was primed using a random-tailed adapter (sm190) in a reaction containing 10 mM Tris (pH 7.9), 10 mM $MgCl_2$, 50 mM NaCl, 1 mM DTT, 2.5 μM primer, 1 mM dNTP, and 5 U Klenow. Duplex DNA was column-purified (DNA Clean & Concentrator-5) before amplification. Libraries were PCR-amplified for 20 cycles using barcode primers (ScriptSeq Index PCR Primers; Epicentre) and primer sm192 in a reaction containing 20 mM Tris (pH 8.8), 10 mM KCl, 10 mM $(NH_4)_2SO_4$, 2 mM $MgSO_4$, 0.1% Triton X-100, 200 μM dNTP, 0.2 μM each primer, and 2.5 U of a 200:1 mixture of Taq and pfu

polymerases. Single-strand DNA was degraded with Exonuclease I. Libraries were separated on 1.5% agarose and column-purified (EZ-10 Spin Column; Bio Basic). Libraries were sequenced on an Illumina HiSeq 2000.

For qPCR, nascent RNA (2.75 μg) was random-primed and reverse-transcribed [50 mM Tris, pH 8.3, 75 mM KCl, 3 mM $MgCl_2$, 5 mM DTT, 0.5 mM dNTP, 2.5 μM primer, 0.3 μg random hexamer, 200 U MMLV-RT]. Quantitative PCR reactions contained 20 mM Tris (pH 8.8), 10 mM KCl, 10 mM $(NH_4)_2SO_4$, 2 mM $MgSO_4$, 0.1% Triton X-100, 200 μM dNTP, 0.5 μM forward and reverse primer (Table S3), 6% ethylene glycol, 0.3× SYBR Green I (Invitrogen), and 0.05 U/μL of Taq polymerase. RNA levels for each gene were normalized to RP49 pre-mRNA.

Determination of Genes Affected by TAF1 Depletion. Two biological replicates of the nascent-seq preparation were performed. Reads were mapped to the *Drosophila* genome using Bowtie allowing two mismatches. Mock-treated libraries had 11,022,632 and 15,408,670 mapped reads and the TAF1 libraries had 8,674,903 and 7,025,140 mapped reads. A gene was called as present at the 0.5 RPKM level. For these S2 cells, we identified 6,436 genes that are present at this level. For genes called up-regulated, the gene must be present in the TAF1 library. For genes called down-regulated, the gene must be present in the mock-treated library. For promoter analysis, the sequence of the 200 bp surrounding the annotated start of each gene was used to create promoter datasets. Each dataset was interrogated using MEME Suite software (40). The sequence motifs defined as specific for each dataset were used to probe a database containing all of the promoters active in these S2 cells. We used FIMO software and a cutoff of *P* value less than 0.0001 (41).

1. Tanese N, Pugh BF, Tjian R (1991) Coactivators for a proline-rich activator purified from the multisubunit human TFIID complex. *Genes Dev* 5(12A):2212–2224.
2. Dynlacht BD, Hoey T, Tjian R (1991) Isolation of coactivators associated with the TATA-binding protein that mediate transcriptional activation. *Cell* 66(3):563–576.
3. Tora L (2002) A unified nomenclature for TATA box binding protein (TBP)-associated factors (TAFs) involved in RNA polymerase II transcription. *Genes Dev* 16(6):673–675.
4. Näär AM, Lemon BD, Tjian R (2001) Transcriptional coactivator complexes. *Annu Rev Biochem* 70:475–501.
5. Chalkley GE, Verrijzer CP (1999) DNA binding site selection by RNA polymerase II TAFs: A TAF(II)250-TAF(II)150 complex recognizes the initiator. *EMBO J* 18(17):4835–4845.
6. Burke TW, Kadonaga JT (1997) The downstream core promoter element, DPE, is conserved from *Drosophila* to humans and is recognized by TAFII60 of *Drosophila*. *Genes Dev* 11(22):3020–3031.
7. Verrijzer CP, Yokomori K, Chen JL, Tjian R (1994) *Drosophila* TAFII150: Similarity to yeast gene TSM-1 and specific binding to core promoter DNA. *Science* 264(5161):933–941.
8. Verrijzer CP, Chen JL, Yokomori K, Tjian R (1995) Binding of TAFs to core elements directs promoter selectivity by RNA polymerase II. *Cell* 81(7):1115–1125.
9. Hsu JY, et al. (2008) TBP, Mot1, and NC2 establish a regulatory circuit that controls DPE-dependent versus TATA-dependent transcription. *Genes Dev* 22(17):2353–2358.
10. Goodrich JA, Tjian R (2010) Unexpected roles for core promoter recognition factors in cell-type-specific transcription and gene regulation. *Nat Rev Genet* 11(8):549–558.
11. Freiman RN, et al. (2001) Requirement of tissue-selective TBP-associated factor TAFII105 in ovarian development. *Science* 293(5537):2084–2087.
12. Tatarakis A, et al. (2008) Dominant and redundant functions of TFIID involved in the regulation of hepatic genes. *Mol Cell* 31(4):531–543.
13. D'Alessio JA, Ng R, Willenbring H, Tjian R (2011) Core promoter recognition complex changes accompany liver development. *Proc Natl Acad Sci USA* 108(10):3906–3911.
14. Deato MD, Tjian R (2007) Switching of the core transcription machinery during myogenesis. *Genes Dev* 21(17):2137–2149.
15. O'Keefe DD, et al. (2012) Combinatorial control of temporal gene expression in the *Drosophila* wing by enhancers and core promoters. *BMC Genomics* 13(1):498.
16. Gegonne A, et al. (2012) The general transcription factor TAF7 is essential for embryonic development but not essential for the survival or differentiation of mature T cells. *Mol Cell Biol* 32(10):1984–1997.
17. Indra AK, et al. (2005) TAF10 is required for the establishment of skin barrier function in foetal, but not in adult mouse epidermis. *Dev Biol* 285(1):28–37.
18. Apone LM, Virbasius CM, Reese JC, Green MR (1996) Yeast TAF(II)90 is required for cell-cycle progression through G2/M but not for general transcription activation. *Genes Dev* 10(18):2368–2380.
19. Martin J, Halenbeck R, Kaufmann J (1999) Human transcription factor hTAF(II)150 (CIF150) is involved in transcriptional regulation of cell cycle progression. *Mol Cell Biol* 19(8):5548–5556.
20. Talavera A, Basilico C (1977) Temperature sensitive mutants of BHK cells affected in cell cycle progression. *J Cell Physiol* 92(3):425–436.
21. Metzger D, Scheer E, Soldatov A, Tora L (1999) Mammalian TAF(II)30 is required for cell cycle progression and specific cellular differentiation programmes. *EMBO J* 18(17):4823–4834.
22. Maston GA, et al. (2012) Non-canonical TAF complexes regulate active promoters in human embryonic stem cells. *Elife* 1:e00068.
23. Marr MT II, Isogai Y, Wright KJ, Tjian R (2006) Coactivator cross-talk specifies transcriptional output. *Genes Dev* 20(11):1458–1469.
24. Aoyagi N, Wassarman DA (2000) Genes encoding *Drosophila melanogaster* RNA polymerase II general transcription factors: Diversity in TFIIA and TFIID components contributes to gene-specific transcriptional regulation. *J Cell Biol* 150(2):F45–F50.
25. Clemens JC, et al. (2000) Use of double-stranded RNA interference in *Drosophila* cell lines to dissect signal transduction pathways. *Proc Natl Acad Sci USA* 97(12):6499–6503.
26. Wright KJ, Marr MT II, Tjian R (2006) TAF4 nucleates a core subcomplex of TFIID and mediates activated transcription from a TATA-less promoter. *Proc Natl Acad Sci USA* 103(33):12347–12352.
27. Spedale G, Timmers HT, Pijnappel WW (2012) ATAC-king the complexity of SAGA during evolution. *Genes Dev* 26(6):527–541.
28. Marr SK, Pennington KL, Marr MT (2012) Efficient metal-specific transcription activation by *Drosophila* MTF-1 requires conserved cysteine residues in the carboxy-terminal domain. *Biochim Biophys Acta* 1819(8):902–912.
29. Celniker SE, et al.; modENCODE Consortium (2009) Unlocking the secrets of the genome. *Nature* 459(7249):927–930.
30. Khodor YL, et al. (2011) Nascent-seq indicates widespread cotranscriptional pre-mRNA splicing in *Drosophila*. *Genes Dev* 25(23):2502–2512.
31. Wuarin J, Schibler U (1994) Physical isolation of nascent RNA chains transcribed by RNA polymerase II: Evidence for cotranscriptional splicing. *Mol Cell Biol* 14(11):7219–7225.
32. Machanick P, Bailey TL (2011) MEME-ChIP: Motif analysis of large DNA datasets. *Bioinformatics* 27(12):1696–1697.
33. Bailey TL, Machanick P (2012) Inferring direct DNA binding from ChIP-seq. *Nucleic Acids Res* 40(17):e128.
34. FitzGerald PC, Sturgill D, Shyakhtenko A, Oliver B, Vinson C (2006) Comparative genomics of *Drosophila* and human core promoters. *Genome Biol* 7(7):R53.
35. Hoffmann A, Oelgeschläger T, Roeder RG (1997) Considerations of transcriptional control mechanisms: Do TFIID-core promoter complexes recapitulate nucleosome-like functions? *Proc Natl Acad Sci USA* 94(17):8928–8935.
36. Yakovchuk P, Gilman B, Goodrich JA, Kugel JF (2010) RNA polymerase II and TAFs undergo a slow isomerization after the polymerase is recruited to promoter-bound TFIID. *J Mol Biol* 397(1):57–68.
37. Raj A, Peskin CS, Tranchina D, Vargas DY, Tyagi S (2006) Stochastic mRNA synthesis in mammalian cells. *PLoS Biol* 4(10):e309.
38. Sims HI, Chirn GW, Marr MT II (2012) Single nucleotide in the MTF-1 binding site can determine metal-specific transcription activation. *Proc Natl Acad Sci USA* 109(41):16516–16521.
39. Nicol JW, Helt GA, Blanchard SG, Jr., Raja A, Loraine AE (2009) The Integrated Genome Browser: Free software for distribution and exploration of genome-scale datasets. *Bioinformatics* 25(20):2730–2731.
40. Bailey TL, et al. (2009) MEME SUITE: Tools for motif discovery and searching. *Nucleic Acids Res* 37(Web Server issue):W202–W208.
41. Grant CE, Bailey TL, Noble WS (2011) FIMO: Scanning for occurrences of a given motif. *Bioinformatics* 27(7):1017–1018.